Revue des Energies Renouvelables Vol. 18 N°4 (2015) 551 – 564

Theoretical and numerical approaches of a plane, laminar and non-confined, impinging jet

A. Aliouali [1], K. Talbi [2] and M. Kadja

Laboratory of Applied Energetics and Pollution
Mechanical Engineering Department
University of Mentouri Brothers, Constantine 1, Algeria

(reçu le 19 Novembre 2015 – accepté le 30 Décembre 2015)

Abstract - *We propose in this paper, a numerical study of a planar impacting jet flow. The flow is assumed isothermal, laminar and unconfined. The developed computer code is based on the finite volume method, which was used to discretize the N-S equations. The code allowed us to simulate the physical phenomenon's taking place in the jet flow. The work focuses, on the description of the evolution of the jet and the presentation of the different characteristics of the flow, for different values of the Reynolds number and the impacting height. Calculations were made for values of the Reynolds numbers ranging from 0.01 to Re = 2000, i.e. in the limits of laminar flow regime, and for values of the ratio between the height of the outlet nozzle-impact surface of 0.1 to 20. The theoretical and numerical approaches of this work are confronted with the experimental works of Sholtz et al.,* [2].

Résumé – *Dans cet article, on vous propose une étude numérique d'un jet plan impactant. Le flux est supposé isothermique, laminaire et non confiné. Le code informatique développé est basé sur la méthode du volume limité utilisée pour numériser les équations N-S. Le code nous a permis de simuler et reproduire le phénomène physique qui se produit dans le flux du jet. Ce travail se concentre sur la description de l'évolution du jet et la présentation des différentes caractéristiques de l'écoulement, pour différentes valeurs données du nombre de Reynolds et de la hauteur de l'impact. Les calculs ont été réalisées sur la base d'un nombre de Reynolds compris entre 0.01 jusqu'à Re=2000, c-à-di dans la limite du régime laminaire du flux, et des valeurs du ratio entre la hauteur de la buse de sortie-la surface d'impact entre 0.1 et 20. Les approches théoriques et numériques de ce travail se confronte aux travaux expérimentaux de Sholtz et al.,* [2].

Key words: Isothermal – Numerical - Plane impacting jet - Laminar.

1. INTRODUCTION

Most of the researches concerning the flow of an impacting jet are devoted to the axisymmetric jet type, emanating from a cylindrical nozzle, the reason being the simplicity in practice. In the laminar regime, the largest number of works is devoted to the influence of the parameters, such as the Reynolds number, the velocity profile in the inlet nozzle and the impact height of the jet on heat and mass transfers. Research works which fall in this category are those published by: Glauert [1], Saad *et al.*, [7], Sparrow *et al.*, [8, 9], Bergthorson *et al.*, [10] and Van Heiningen *et al.*, [11].

Among the studies of unconfined and isothermal configurations, similar to ours, is that of Sholtz *et al.*, [2]. It includes theoretical and experimental work of an air jet impacting on a flat plate. For their theoretical study the jet flow in the nozzle is assumed, non-viscous and rotational and in the region near to the impact surface, it obeys the law of boundary layers. The experimental data measured in the nozzle by these authors, have been verified by the theoretical model of non-viscous fluids.

[1] Abdelaliouali843_@gmail.com
[2] kam.talbi@gmail.com

Furthermore, they found that there is a depression located on the wall at the exit of the nozzle, due to the viscosity when Re is small. According to the comments of Sholtz *et al.*, [2], the flow along the impact surface resulting from the jet tends to detach from the impact surface and return toward the jet with the formation of fluid recirculation cells at low Reynolds numbers.

In the domain of numerical resolution, difficulties appear during the boundary conditions implementation at the exit boundaries of the calculation domain and at the free boundaries because of the non confinement of the jet. Yuan *et al.*, [3] as well as Mikhail *et al.*, [4] imposed zero gradients as boundary conditions. Wang *et al.*, [5] considered the same configuration and in order to obtain a model close to reality, the authors proposed new boundary conditions. Thus by imposing zero axial velocity, they managed to get the lateral velocity from the continuity equation.

The jet type in our study is the plane jet which can be considered as a fundamental and academic research flow. It has wide technological applications in several industrial domains such as drying, cooling, heating, ventilation, air conditioning, in aerospace and in air curtain devices. The work that we are presenting here fits in this context. It consists of theoretical and numerical approaches for the study of the evolution of the jet flow under the influence of two parameters: the Reynolds number and the impact height.

2. PROBLEM FORMULATION

2.1 Assumptions

We here consider an incompressible, permanent, isothermal, flow of a plane laminar air jet. All the physical properties of air, which was assumed Newtonian, are constant and the viscous dissipation is negligible. Theoretically in a first approach, our jet can be defined as the result of a jet of air through a rectangular cross-section which has a width of $2X_0$ and a length assumed very large as compared to the width, which allows to overlook the effects of edges, and to set the azimuthal velocity to zero so the problem can be assumed two-dimensional and perfectly symmetrical with respect to the nozzle axis (figure 1). As an infinite domain approach, we have chosen a finite domain, sufficiently large compared to the nozzle width ($2X_0$) and such that the nozzle exit is separated from the impact surface by a distance H.

2.2 Governing equations

By setting the reference values equal to those at the nozzle inlet, we can define the following dimensionless variables:

$$x^*=x/X_0\ ,\ y^*=y/X_0\ ,\ u^*=u/V_{max\,0}\ ,\ v^*=v/V_{max\,0}\ ,$$

$$\rho^*=\rho/\rho_0\ ,\ \mu^*=\mu/\mu_0\ \text{ et }\ p^*=(p-P_0+\rho_0 g)/(\rho_0 V_{max\,0}^2)$$

The dimensionless equations governing the flow can then be written in the following form:

$$\frac{\partial u^*}{\partial x^*}+\frac{\partial v^*}{\partial y^*}=0$$

$$u^*\frac{\partial u^*}{\partial x^*}+v^*\frac{\partial u^*}{\partial y^*}=-\frac{\partial p^*}{\partial x^*}+\frac{1}{Re.}\left(\frac{\partial^2 u^*}{\partial x^{*2}}+\frac{\partial^2 u^*}{\partial y^{*2}}\right)$$

$$u^*\frac{\partial v^*}{\partial x^*} + v^*\frac{\partial v^*}{\partial y^*} = -\frac{\partial p^*}{\partial y^*} + \frac{1}{Re}\left(\frac{\partial^2 v^*}{\partial x^{*2}} + \frac{\partial^2 v^*}{\partial y^{*2}}\right)$$

In these equations, we observe a single dimensionless parameter: the Reynolds number Re. Taking into account the jet geometry which is characterized by the width X_0 and the distance H separating the nozzle exit from the impact surface, the isothermal plane jet can perfectly be characterized by the following two dimensionless parameters: Re and H/X_0.

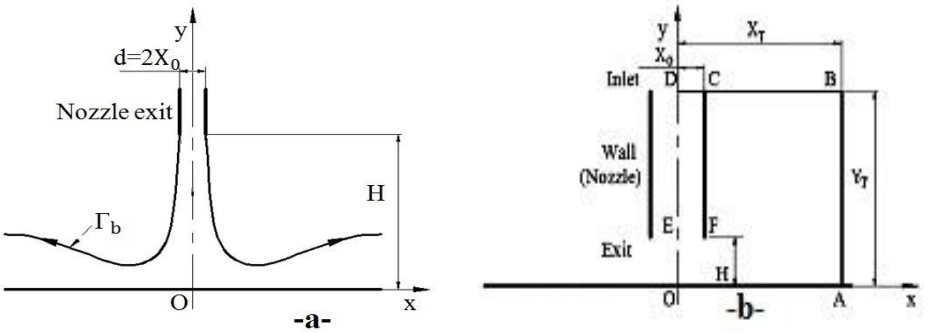

Fig. 1: **-a-** Border streamline Γ_b and **-b-** Representation of the computational domain

2.3 Boundary conditions

Normally, there is no flow at the domain exit boundaries BC and AB, because the jet is unconfined. Therefore on these boundaries, we have considered the real fluid non-slip conditions, i.e. $u = v = 0$. However this is not possible, because the continuity equation is not satisfied. In order to remedy for this, Wang *et al.*, [5] proposed, new conditions. For our case, we have adopted them:

On BC: $u = 0$ and $\frac{\partial v}{\partial y} = 0$. The pressure then takes the ambient value, $p = P_0$.

On AB: the lateral velocity u is deducted from the continuity equation and the axial velocity is zero, $v = 0$, $p = P_0$.

On DC: $v = V_{max\,0}$, $v = V_{max\,0}\cdot\left(1 - \left(\frac{x}{X_0}\right)^2\right)$

On CF and OA: $u = 0$ and $v = 0$

On OD: $u = 0$, $\frac{\partial v}{\partial x} = 0$

2.4 The numerical resolution method

The numerical resolution of the set of partial differential equations governing the flow is ensured by the finite volume method and by using the Simpler algorithm proposed by Patankar [6] for pressure-velocity coupling. The mesh used in the computations is non-uniform and structured. Given the symmetry of the problem, we only considered half of the domain determined by the rectangular section noted ($X_T \times Y_T$).

The convergence of the overall solution is considered to be reached when the total mass residual of the fluid in the field is less than 10^{-4} % the mass flow at the entrance of the nozzle. The influence of the size of the study domain and the number of points in the mesh were investigated by considering as criteria, the maximum lateral velocity U_{max} and the maximum stream function value Ψ_{max} □, in the computational field. The results of this preliminary investigation are grouped in **Table 1**. We note that the criteria values at the chosen different calculation conditions are very close to each other. In order to minimize the computational time we chose the study size ($51X_0 \times 58X_0$) and the number of nodes in the mesh size (31 x 31) for all remaining computations. We have adopted the reference state, $Re = 100$ and $H/X_0 = 8$.

Table 1: Maximal lateral velocity and its location in the whole calculation domain, for $Re = 100$ and $H/X_0 = 8$

Calculation domain size	**Mesh grids**	U_{max} □$/V_{max\,0}$	**Location of** U_{max} □		Ψ_{max}
			x/X_0	y/X_0	
$131X_0$ x $138X_0$	31 x 31	0.6648	2.8416	0.5282	3.3354
$121X_0$ x $128X_0$	31 x 31	0.6647	2.8244	0.5282	3.2757
$111X_0$ x $118X_0$	31 x 31	0.6646	2.8059	0.5282	3.2104
$51X_0$ x $58X_0$	31 x 31	0.6645	3.1205	0.5282	2.6678
$51X_0$ x $58X_0$	41 x 41	0.6661	3.0947	0.5282	2.6555
$51X_0$ x $58X_0$	51 x 51	0.6663	3.09719	0.5282	2.6515

3. RESULTS

3.1 Evolution of the jet as a function of the Reynolds number

In the nozzle, because the velocity profile does not vary significantly between the entry and the exit for $Re = 100$ (curve 3 corresponding to $H/X_0 = 8$ in figure 2), the flow of the fluid must obey the Poiseuille plane law for a fully developed laminar flow between two fixed planes. For a developed Newtonian fluid whose profile is parabolic in shape, the theoretical pressure loss between the entry and the exit of the nozzle, i.e. $(-\Delta p = (P_{inj} - P_{ej}))$, is given in dimensionless form by:

$$\left(\frac{P_{inj} - P_{ej}}{H_b}\right).\left(\frac{X_0}{\rho_0 . V_{max\,0}^2}\right) = \frac{2}{Re}$$

Our calculations are performed in a very large Reynolds number interval which stretches from 0.01 to 2000 which is almost the limit of the laminar flow. In figure 3, we find a good agreement between the theoretical and the calculated values and the flow in the nozzle verifies Poiseuille law.

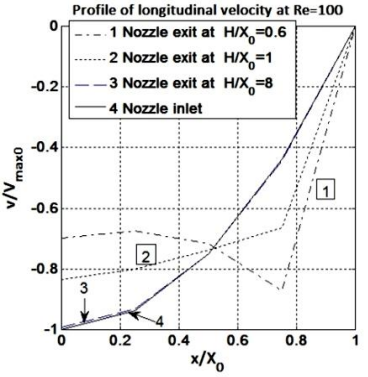

Fig. 2: Profile of velocity v for various values of H/X_0

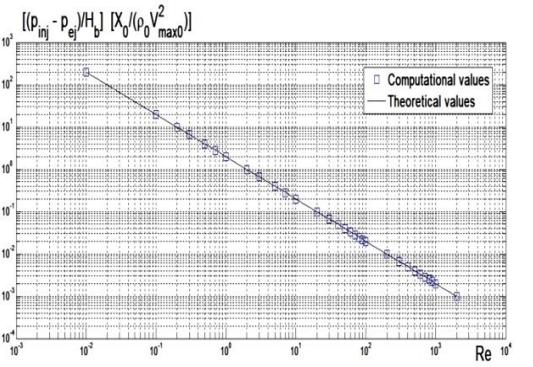

Fig. 3: Pressure loss $(P_{inj}-P_{ej}/H_b)\left(X_0/\rho_0 v_{max\,0}^2\right)$ for $H/X_0=8$

From the nozzle exit onwards a perfect (or non-viscous) fluid, must obey Bernoulli law of mechanical energy conservation between two points. Considering points 1 and 2 on the central streamline, point 1 being located at the exit of the nozzle, where $V_{ej}/V_{max\,0=1}=1$ and point 2 at the interface of the impact surface, where $V_s/V_{max\,0=0}=1$, we deduce:

$$\left(\frac{p_s-p_{ej}}{\rho_0 \cdot V_{max\,0}^2}\right)=0.5$$

Mechanical energy is not preserved for a real fluid due to the viscous losses. Curve **2** in figure 4, shows us that in fact (p_s-p_{ej}), is largely negative when Re is less than 10 where viscosity plays a very important role even in the free part of the jet. The pressure at the nozzle exit is therefore superior to that of the impact surface; it is this difference in pressure which pushes the fluid to the impact surface by overcoming the viscous force. The value of (p_s-p_{ej}) becomes positive when Re exceeds 10, and tends towards 0.5 when Re is very important. The fluid behavior in the free zone therefore approaches that of a perfect fluid when Re increases.

Also, in their study of impinging round jets, Sholtz *et al.*, [2] found that there is a depression in the vicinity of the jet because of the high viscosity when Re is small. Let P_{min} □ be the algebraic minimum pressure value in the whole calculation domain. Curve **1** in figure 4, shows the evolution of P_{min} □ as a function of Re. The location of this minimum corresponds to the center of the depression. This depression center is located on the wall at the exit of the nozzle up to $Re=500$. It moves progressively towards the impact surface for values of Re greater than 500. The absolute value of P_{min} □ decreases very rapidly with Re.

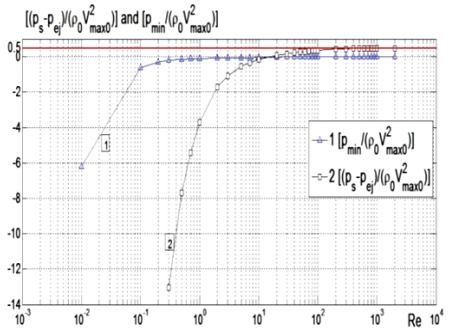

Fig. 4: Pressure differences $(P_s - P_{ej}/\rho_0 V^2_{max\,0})$ and $(P_{min}/\rho_0 V^2_{max\,0})$ versus Re for $H/X_0 = 8$

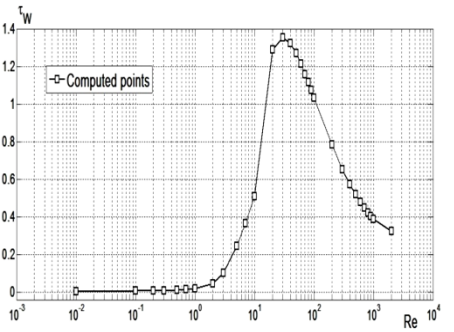

Fig. 5: τ_W versus to the Reynolds number for $H/X_0 = 8$

From the exit of the nozzle onwards, the projected fluid begins to interact with the surrounding air. The amount of entrained air is characterized by the entrainment rate τ_W, defined by: $\tau_w = \dfrac{W_{max}}{W_0} - 1.$

Or by the equivalent equation using the stream function: $\tau_w = \dfrac{\Psi_{max}}{\Psi_0} - 1.$

In figure 5, we find that the rate of entrainment τ_W increases very slowly at low Reynolds numbers. From $Re = 1$ onwards, τ_W undergoes a remarkable progress, and reaches its maximum at $Re = 30$. After this critical point, τ_W decreases with the Reynolds number. The increase of Re, leads to two opposite effects on the amount of entrained gaz, due to the increase of the force of inertia with Re. The velocity on the border stream line Γ_b -which separates the projected fluid and the entrained fluid- increases, which tends to reinforce the entrainment. Also, the viscosity becomes less and less important than the force of inertia when Re increases. The development of the boundary layer is therefore less pronounced thereby reducing the flow induced around the jet. These two opposite effects are responsible for the maximum observed for τ_W when Re is in the vicinity of 30.

The flow along the impact wall resulting from the jet impact tends, in accordance with the observations of Sholtz *et al.*, [2], to take off from the impact surface because of the depression and to return towards the jet with the formation of recirculation cells. The same behavior is observed at low Reynolds numbers (0.01 to 300). Indeed the results presented in figures 6-**a**, **-b**, **-c**, **-d**, and **-f**; correspond to low Reynolds numbers comprised between 0.01 and 300. Fluid recirculation regions are observed. In such domains the increase of the Reynolds number leads to a very rapid increase of the velocity on the border streamline Γ_b. The size of the domain of the entrained fluid increases and induces a more important entrainment of the neighboring fluid.

From $Re = 300$ onwards, the recirculation phenomena are no longer observed. In figures 7-**a**, **-b**, and **-c**, the recirculation regions disappear, and this limit is in perfect agreement with the observations of Sholtz *et al.*,[2].

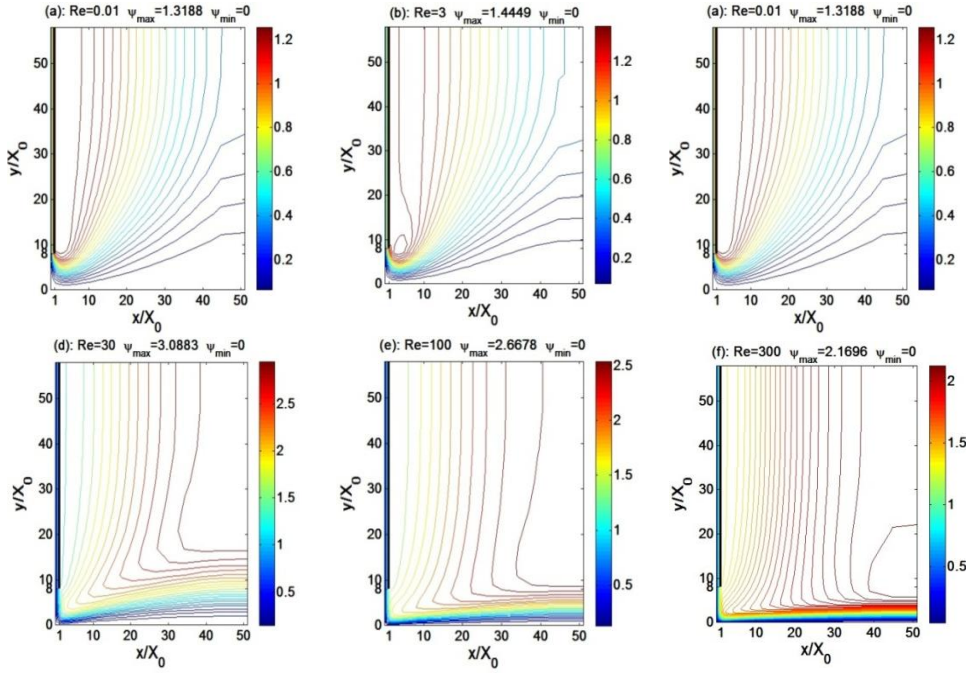

Fig. 6: Streamlines at low Reynolds numbers for $H/X_0 = 8$, observation of the recirculation regions

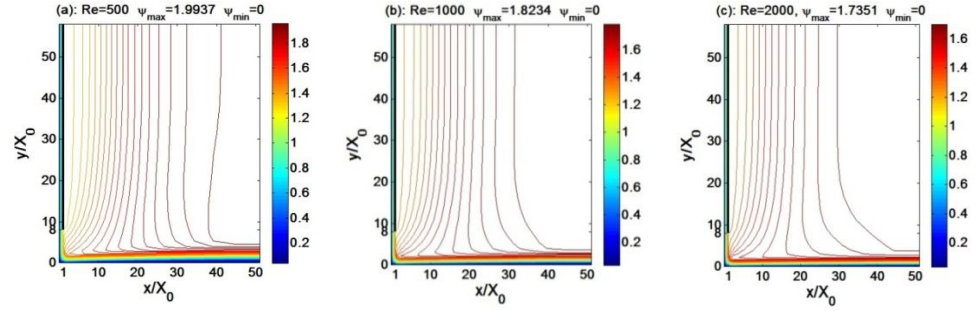

Fig. 7: Streamlines at high Reynolds numbers for $H/X_0 = 8$, absence of the recirculation regions

In figures 8-**(a-1)** and 8-**(a-2)**, we can notice that the axial velocity v remains almost constant inside the nozzle up to the opening (which corresponds to $y = 8X_0$) because of the constraint imposed at the wall. From this point onwards, the situations differ in function of the Reynolds number.

At low Reynolds numbers, in practice when $Re \leq 10$, v undergoes a sudden drop (curve **1**, in figures 8-**(a-1)** and 8-**(a-2)**). Here occurs the creeping flow of the fluid which changes from the axial direction to the lateral direction at $y = 7X_0$, while the lateral velocity u already takes its maximum value (curve **1** in figures 9-**(b-1)** and 9-**(b-2)**). Then follows the very thick boundary layer up to the wall.

When Re increases, the core -corresponding to a value of the velocity v nearly equal to that of nozzle- appears, as can be clearly noticed on curve 5 in figures 8-**(a-1)** and 8-**(a-2)**. At the same time, the maximum of the velocity u grows (the curve **5** in

figure 9-**(b-1)** and 9-**(b-2)**) and its position becomes closer to the wall, resulting in a decrease in the thickness of the boundary layer.

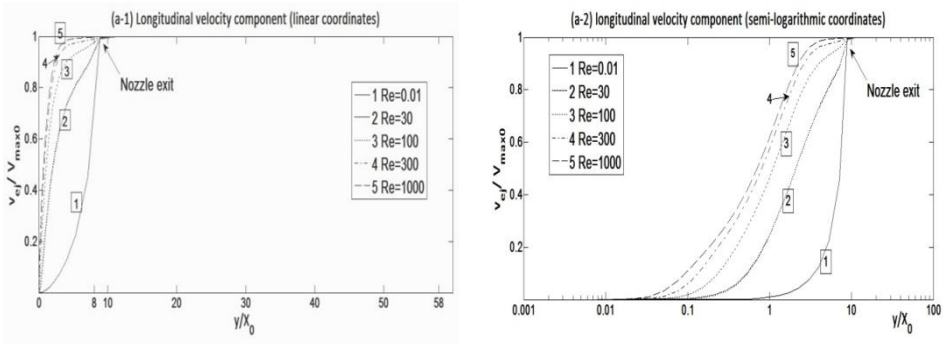

Fig. 8: Evolution of v versus the distance (y/X_0)
for different Reynolds numbers and $H/X_0=8$

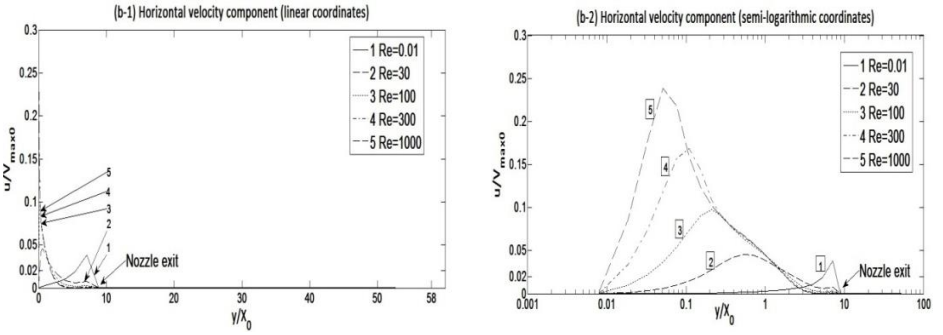

Fig. 9: Evolution of u versus the distance (y/X_0)
for different Reynolds numbers and $H/X_0=8$

3.2 Evolution of the jet as a function of the nozzle-impact surface distance

In figure 10, we see the evolution of the influence of the distance (H/X_0) - separating the nozzle from the impact surface- on the jet characteristic velocities, U_{max} □ and V_{ej}. The velocity U_{max} □ varies considerably with H. On curve **1**, we find that the ratio (U_{max} □/ $V_{max\,0}$) may exceed unity when (H/X_0) is very small. In this case, the velocity profile is no longer parabolic at the nozzle exit. At the exit of the nozzle, the central velocity V_{ej} is less than $V_{max\,0}$ as shown by curve 2 in Figure 10 and there is a flattened profile. When $H/X_0 \geq 2$ the velocity U_{max} □ decreases slightly, while V_{ej} the velocity approaches increasingly the $V_{max\,0}$ value.

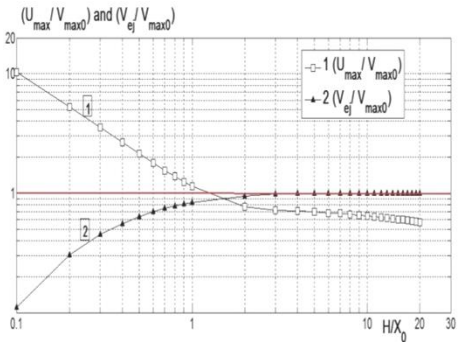

Fig. 10: U_{max} □ and V_{ej} versus H/X_0 for $Re = 100$

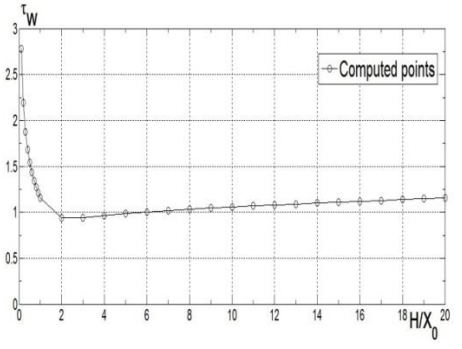

Fig. 11: τ_W versus H/X_0 for $Re = 100$

Figure 11 shows the entrainment rate as a function of (H/X_0). This entrainment rate is directly proportional to (H/X_0) at high values of (H/X_0). But if the nozzle is brought closer to the impact surface there will be an increase in lateral velocity and the latter can reach values greater than the maximum value in the nozzle inlet $V_{max\,0}$ (see figure 10). This phenomenon is responsible for a more important entrainment of the fluid in the neighbourhood. A growth of τ_W with the decrease of (H/X_0) is therefore noticed when (H/X_0) is less than 2.

Figure 12 illustrates the evolution of the pressure difference ($p_{1s} - p_{ej}$) as a function (H/X_0). As shown in figure 10, the maximum velocity V_{ej} at the exit of the nozzle is very close to $V_{max\,0}$ when (H/X_0) is high, and decreases with the nozzle - impact surface distance. This implies that the kinetic energy available at the exit of the nozzle and which is convertible into pressure on the impact surface- increases with (H/X_0). At the same time, the viscous loss between the nozzle and the impact surface is directly proportional to the distance (H/X_0).

These two opposite effects are responsible for the change in the evolution of ($p_{1s} - p_{ej}$) recorded in the domain for values of (H/X_0) in the interval 0.1 to 2.

Beyond the value (H/X_0) = 2, we notice, whatever the Reynolds number, the viscous loss remains directly proportional to the distance (H/X_0). At low values of the Reynolds number Re ≤ 30, where viscosity has a very important effect, viscous loss exceeds the kinetic energy possessed by the fluid at the nozzle exit and therefore ($p_{1s} - p_{1ej}$) < 0, i.e. the motor pressure on the impact surface is lower than that at the nozzle exit.

It decreases with increasing Reynolds number and for $Re \geq 808$, it becomes close to the theoretical limit for a perfect fluid: $\left(\frac{p_s - p_{ej}}{\rho_0 \cdot V_{max\,0}^2} \right) = 0.5$. These results are consistent with the experimental data measured by Sholtz *et al.*, [2], and lead to the conclusion that the fluid is practically non-viscous for Re greater than 808.

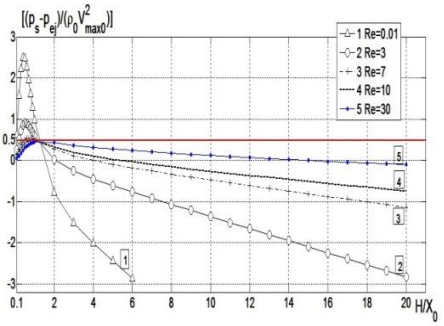

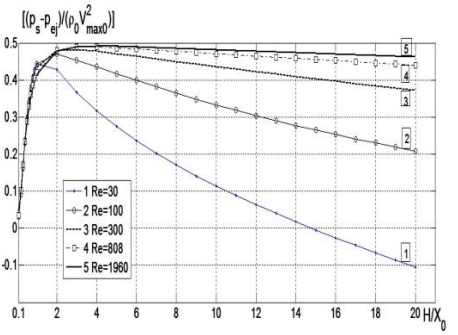

Fig. 12: Pressure differences $\left(\frac{p_s - p_{ej}}{\rho_0 . V^2_{max\,0}} \right)$ versus H/X_0 and Re

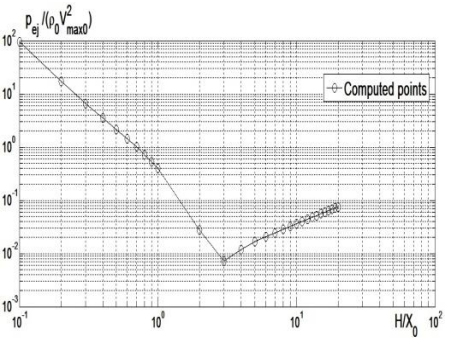

Fig. 13: versus $\left(P_{ej} / \rho_0 . V^2_{max\,0} \right)$ H/X_0 for $Re = 100$

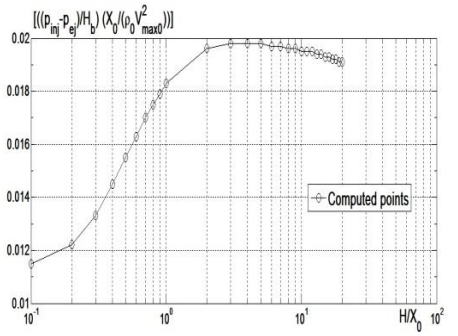

Fig. 14: $\left(\frac{p_{inj} - p_{ej}}{H_b} \right) \left(X_0 / \rho_0 . V^2_{max\,0} \right)$ versus H/X_0 for $Re = 100$

Figure 13 summarizes the evolution of the motor pressure P_{ej} at the exit of the nozzle. For small values of (H/X_0), P_{ej} reaches a very important value compared to the kinetic energy $(\rho_0 . V^2_{max\,0})$. This high value of P_{ej} is justified for small values of (H/X_0), by the lateral acceleration of the fluid which converts pressure energy into kinetic energy. The pressure P_{ej} is practically zero for (H/X_0) values greater than 2. While we see a slight rise due to the increasing viscous loss with (H/X_0).

The dimensionless viscous friction loss $\left(P_{inj} - P_{ej} / H_b \right) \left(X_0 / \rho_0 . V^2_{max\,0} \right)$, between the nozzle entrance and its exit is also sensitive to the nozzle - impact surface distance. Figure 14 shows this evolution for $Re = 100$. When (H/X_0) is very low, the pressure loss in the nozzle is much smaller than 0.02, which is the value estimated by Poiseuille model. The difference between the two calculations becomes low when

(H/X_0) is greater than 2. But we see a slight increase when (H/X_0) is high, this is due to the growing viscous loss with (H/X_0).

Another dynamic feature of the jet is the pressure loss coefficient, defined by Sholtz *et al.*, [2] as:

$$\beta = \frac{P_n - p_a}{\rho_0 U^2}$$

where, $p_a = 0$, Motor ambient pressure en [Pa], p_n, Non-perturbed motor pressure inside the nozzle en [Pa] and $U = 2/3V_{max\,0}$, Mean velocity at the nozzle entrance [m/s].

As defined by Sholtz *et al.*, [2], the coefficient β is function of impact height (H/X_0) and the Reynolds number Re, due, respectively, to the constriction of the flow and viscous loss at the nozzle exit. The results are presented in figure 15, where we find, depending on the height of impact, the coefficient β reaches a very high value when (H/X_0) is small. This is justified by the importance of the constriction. However β is lower for $(H/X_0) \geq 2$, but a slight rise can be seen due to the increase of the viscous loss with (H/X_0).

As a function of Reynolds numbers and for low Re values such as $Re = 100$, we notice a β value more important than that at $Re \geq 808$. This is due to the preponderant influence of viscous loss, at $Re = 100$, from the nozzle exit onwards. For $Re \geq 808$, as indicated in figure 12, the fluid can be considered perfect in this case, and hence the pressure loss coefficient β would be independent of the Reynolds number. Indeed as can be seen in figure 15, the values of the coefficient β are very close. Because of the very low influence of viscosity on jet flow, the pressure loss coefficient β takes the value corresponding to the theoretical limit for a perfect fluid. Sholtz *et al.* [2] arrived at the same conclusion for a circular jet.

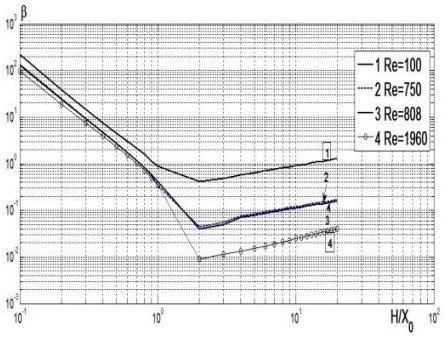

Fig. 15: β versus H/X_0 for different Reynolds numbers.

4. CONCLUSION

In this work, we developed a computer code in a two-dimensional domain for the resolution of the problem of the plane impinging jet. The flow is assumed to be laminar and isotherm. The configuration is non-confined. By making a suitable choice of the boundary conditions, because of non-confinement, the accuracy of solutions is

satisfactory and the size of the computational domain has very little influence on the velocity field.

Our results are validated using the Poiseuille plane model in the nozzle and show that the effect of viscosity on jet flow is small when the Reynolds number $\mathrm{Re} \geq 808$. This allows us to consider the jet flow at $\mathrm{Re} \geq 808$ practically as an inviscid fluid flow. Sholtz *et al.*, [2] arrived at the same conclusion for a circular jet.

At low Reynolds numbers recirculation cells are created due to the depression. While they are absent, for Reynolds numbers greater than $\mathrm{Re} = 300$. When the Reynolds number is less than 30 and due to the viscous behavior of the fluid, between the exit of the nozzle and the impact surface, viscous friction loss exceeds the kinetic energy possessed by the fluid at the nozzle exit, so that ($P_s - P_{ej} < 0$), Which makes the motor pressure on the impact surface lower than that at the nozzle exit.

For very low distances between the nozzle exit and the impact surface ($H/X_0 \leq 2$), the flow is modified up to the inside of the nozzle. The axial velocity profile which no longer follows the Poiseuille model is no longer parabolic, but becomes more and more flattened and the viscous loss becomes less and less important. Whereas for the heights ($H/X_0 \geq 2$), the presence of the impact surface has very little influence on the behavior of upstream flow.

Whatever the Reynolds number, the viscous loss is directly proportional to the distance (H/X_0). It decreases with increasing Reynolds number and approaches the theoretical limit for the perfect fluid.

NOMENCLATURE

$d = 2X_0$, Width of the nozzle [m]	g, Universal acceleration
H, Distance nozzle-impact surface [m]	P, Thermodynamic pressure [Pa or atm]
$H_b = H_T - H$, Length of the nozzle considered in the calculation [m]	H_T, Height of the total calculation domain [m]
P_a, 1 [atm] = 1.01325 10^5 [Pa], Atmospheric pressure	P_0, Fluid thermodynamic pressure at static state [Pa or atm]
p, Motor pressure [Pa]	$p_a = 0$, Ambient motor pressure [Pa]
P_{ej}, Pressure at the point of discharge (on the axis Oy at the exit of the nozzle)	P_{inj}, Motor pressure at the nozzle entrance [Pa]
P_n, Non-perturbed motor pressure in the interior of the nozzle [Pa]	P_s, Motor pressure on the surface of impact [Pa]
P_{min} □, Algebraic minimal pressure in all the calculation field [Pa]	$U = 2/3 V_{max\,0}$, Mean velocity at the nozzle entrance [m/s]
u, Lateral velocity component [m/s]	Re, Reynolds number
U_{max} □, Maximal lateral velocity defined in the whole calculation domain	V_{ej}, Axial central discharge velocity at the exit of the nozzle [m/s]
$V_{max\,0}$, Maximal velocity at the entrance to the nozzle [m/s]	V_s, Axial velocity at the interface of the impact surface [m/s]
$\vec{V}$, Vector velocity of the flow jet [m/s]	v, Axial component of the velocity
W_0, Initial mass flow of air to the inlet nozzle [kg/s]	W_{max} □, Maximal mass flow rate of air in the calculated field [kg/s]

x , Space coordinate lateral direction x	W , Mass flow [kg/s]
Y_T , Total axial dimension of the computational domain [m]	X_T , Total lateral dimension of the computational domain [m]
X_0 , Half the width of the nozzle [m]	y , Space coordinate axial direction y, m
0, in the matter of the inlet nozzle	*, in the matter of the dimensionless value
β , Pressure loss coefficient	μ, Dynamic viscosity [kg/(m.s)]
Γ_b , Line boundary between the fluid projected by the nozzle and the leads	μ_0 , Dynamic viscosity value at the entrance to the nozzle [kg/ (m.s)]
ρ_0 , Density value at the nozzle entrance [kg/m^3]	τ_W , Rate of the surrounding air, training without unit
Ψ , Non-dimensional stream function value in the whole plotted domain	Ψ_{max} □, Maximal stream function value in the whole plotted domain
Ψ_{min} □, Minimal stream function value in the whole plotted domain	$Re = (\rho_0 X_0 V_{max\,0}) / \mu_0$
Ψ_0, Value of Ψ on the nozzle wall	ρ , Density [kg/m^3]

REFERENCES

[1] M.B. Glauert, '*The Wall Jet*', Journal of Fluid Mechanics, Vol. 1, N°6, pp. 625 – 643, 1956.

[2] M.T. Sholtz and O. Trass, '*Mass Transfer in a Non-Uniform Impinging Jet*', AICHE Journal, Vol. 16, N°1, pp. 82 – 96, 1970.

[3] T.D. Yuan, J.A.Liburdy and T.Wang, '*Buoyancy Effects on Laminar Impinging Jets*', International Journal Heat Mass Transfer, Vol. 31, N°10, pp. 2137 – 2145, 1988.

[4] S. Mikhaïl, S.M. Morcos, M.M.M. AbuI-Ellail and W.S. Ghaly, '*Numerical Prediction of Flow Field and Heat Transfer From a Row of Laminar Slot Jets Impinging on a Flat Plate*', Proceedings of the Seventh International Heat Transfer Conference Vol. 3, pp. 337 – 382, 1982.

[5] Y.B. Wang, C. Chaussavoine and F. Teyssandier, '*Two-Dimensional Modeling of a Non-Confined Circular Impinging Jet Reactor Fluid Dynamics and Heat Transfer*', International Journal of Heat and Mass Transfer, Vol. 36, N°4, pp. 857 - 873, 1993.

[6] S.V. Patankar, '*Numerical Heat Transfer and Fluid Flow*', Mc Graw –Hill, New York, 1980.

[7] N.R. Saad, W.J.M. Douglas and A.S. Mujumdar, '*Prediction of Heat Transfer Under an Axisymmetric Laminar Impinging Jet*', Industrial & Engineering Chemistry Fundamentals, Vol. 16, pp. 148 – 154, 1977.

[8] E.M. Sparrow and L. Lee, '*Analysis of Flow Field and Impingement Heat/Mass Transfer Due to a no Uniform Slot Jet*', Journal of Heat Transfer, Vol. 97, pp. 191 – 197, 1975.

[9] E.M. Sparrow and T.C. Wong, '*Impingement Transfer Coefficients due to Initially Laminar Slot Jets*', International Journal of Heat and Mass Transfer, Vol. 18, pp. 597 – 605, 1975.

[10] J.M. Bergthorson, K. Sone, T.W. Mattner, P.E. Dimotakis, D.G. Goodwin, and Dan I. Meiron, '*Impinging Laminar Jets at Moderate Reynolds Numbers and Separation Distances*', California Institute of Technology, USA, Physical Review E, pp. 1 - 12, 2005.

[11] A.R.P. Heiningen, A.S. van, Mujumdar and W.J.M. Douglas, '*Numerical Prediction of the Flow Field and Impingement Heat Transfer Caused by a Laminar Slot Jet*', Journal of Heat Transfer, Vol. 98, N°4, pp. 654 – 658, 1976.